International Journal of Mechanical Engineering and Robotics Research

ISSN 2278 – 0149 www.ijmerr.com
Vol. 3, No. 3, July 2014

Research Paper

ROOF STRENGTH ANALYSIS OF A TRUCK IN THE EVENT OF A ROLLOVER

Daniel Esaw[1]* and A G Thakur[1]

Corresponding Author:* **Daniel Esaw ✉ *esaw.daniel@mahindraengg.com*

In an event of a rollover of any vehicle , there are fatal injuries to the driver and passenger. Regulation & standards for **FMVSS 216 and ECE R29** takes into the tests the cabin for roof strength. The roof strength is done is two ways either by quasi static or dynamic. This dissertation focuses on the rollover phenomenon by the quasi static approach. There is very little difference in results between quasi static and dynamic rollover. An un laden truck is used to simulate the rollover. A side platen is impacted to simulate the phase-1 of the rollover. Energy depending on the mass of the vehicle is imparted in phase-1. Phase I will end once this energy is completely absorbed by the cab. The phase-1, the cab mounts play an important role as the complete load is transferred to the frame . the cab mounts has a tendency to fail in this phase. In phase II the truck axle weight is given the load to the cab. Per **FMVSS 216 and ECE R29** the load is ramped to 105% of the actual load. A 50th percentile dummy is used to check the intrusion of the cab into the survival space. Force versus displacement is plotted to analyze the strength of the cab. Energy plots will the component which has absorbed the maximum energy. The strain plots of the roof, back panel, floor, cab mounts are plotted and analyzed. After this whole exercise the cab is predicted to pass **FMVSS216 or ECE R29** to have enough strength to withstand a rollover.

Keywords: Roof Strength analysis, Quasi static approach, Dynamic rollover

INTRODUCTION

In the early 1970's, the National Highway Traffic Safety Administration NHTSA) was responsible for the United States becoming the first country in the world to address deaths and serious injures associated with vehicle roof crush. Federal Motor Vehicle Safety Standard (FMVSS) No. 216, "Roof Crush Resistance," became effective on September 1, 1973. This standard established strength requirements for the roof structure over the front occupants of passenger cars with a gross vehicle weight rating (GVWR) of 6,000 pounds or less. The purpose of the standard is to reduce deaths and injuries due to crushing of the roof into the passenger compartment area in rollover crashes. Since 1973, Canada and Saudi Arabia have

[1] Sanjivani Rural COE, Kopargoan, University of Pune.

adopted roof crush standards that have the same requirements as Standard No. 216. We are not aware that any other country has adopted a roof crush standard, and know that both Europe and Japan do not have any such requirements. Since inception, the roof crush standard has been amended, extending its requirements to passenger cars, trucks, buses, and multipurpose passenger vehicles with a GVWR of 2722 kilograms (6000 pounds) or less (55 FR 15510, April 17, 1991). The standard was also amended to modify the test device placement procedure to accommodate vehicles with raised and highly sloped (aerodynamic) roof structures (64 FR 22567, April 27, 1999). The test procedure currently used to evaluate compliance with the standard involves securing a vehicle on a rigid horizontal surface, placing a flat steel rectangular plate on the vehicle's roof, and using the plate to apply 1.5 times the unloaded weight of the vehicle (up to a maximum of 22,240 N, or 5,000 pounds, for passenger cars) onto the roof structure. During the test, the plate is angled and positioned to simulate vehicle-to-ground contact on the roof over the front seat area. To achieve this contact, the plate is tilted forward at a 5-degree angle, along its longitudinal axis, and tilted outward at a 25-degree angle, along it lateral axis, so that the plate's outboard side is lower than its inboard side. The test plate's edges are also positioned with respect to fixed locations on the vehicle's roof, depending upon the roof slope, to ensure that the plate stresses the roof over the front seat area. Compliance with the standard is achieved if the vehicle's roof prevents the test plate from moving downward more than 127 mm (5 inches).

FE MODEL PREPARATION

Cad Data Review

The cad data received from Team centre in UG software is reviewed. The surface features were trimmed and geometry cleaned up for the FEM modeling. The surface is trimmed in such a way that the mesh generated will give carline mesh. Unwanted or duplicate surfaces are deleted which does not allow the mesh to be created. The class of the surface is checked and also its continuity also checked.

Holes below 6mm are plugged i.e. a new surface is created in the place of the whole and the surface now looks as if there were no holes before. The hole below 6 mm does not contribute to the results and hence they are not required considering the whole cab. These bolts are captured by using a centre node at the bolt location.

The assembly of the cab checked is as follows

a) Cab in white (CIW)

b) Roof structure

c) Cab Mount both front and rear

d) Door assembly

Figure 1: FE Mesh Model of CIW as Well as the Door

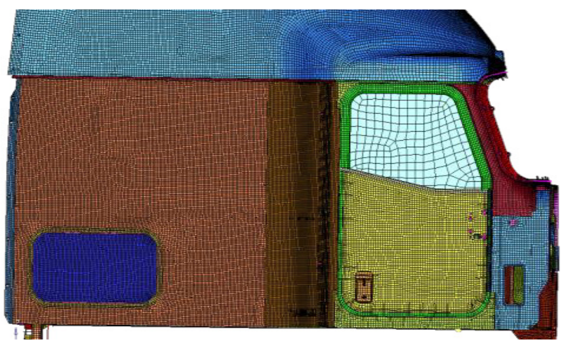

Finite Element Modeling of the Complete Cab

The cad model after geometry clean-up is then taken up for meshing. In meshing the component is modeled with element size as per the requirement of the solver. For steel the minimum element size is 5 mm, but as the features of the parts needs to be captured it is not possible to maintain an element length of 5mm so the elements can go up to a minimum of 3 mm. The least element size is maintained at 3mm, so that it does not affect the solver time (Figure 2).

Figure 2: FE Model with Front Cab Frame

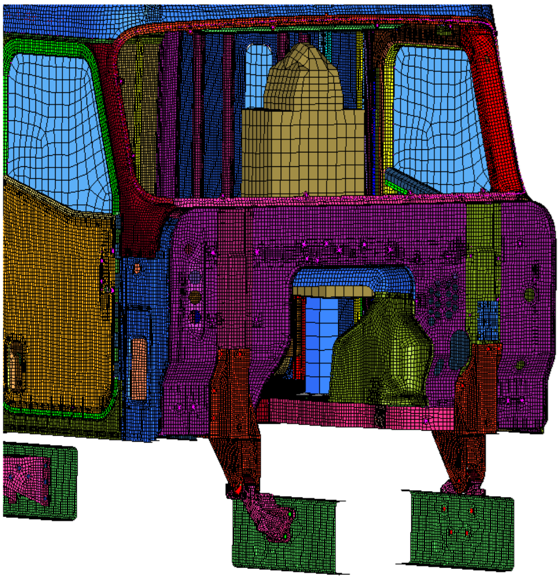

FE Model With Front Cab Frame

The individual component is meshed and then assembly as per sub-assembly.

The assembly tree so created helps in locating the part per its sub system.

The sub-system created are as follows

a) Cab in white (CIW)

b) Roof structure

c) Cab Mount both front and rear

d) Door assembly

e) Interior and trims

f) Glass and windows

Figure 3: 50th Percentile Dummy Details

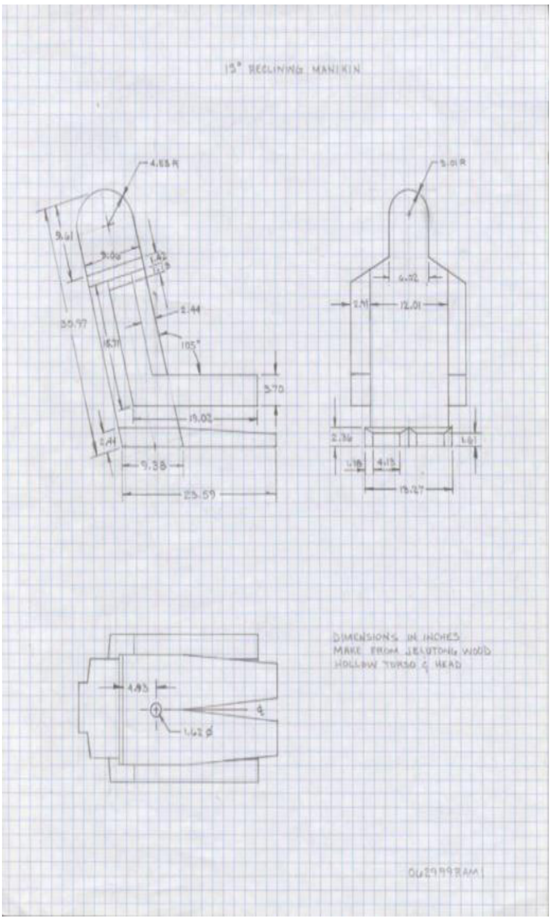

Geometric and Material Properties

The complete FE model is assigned geometric as well as material properties in Hypermesh. The thickness of the component is given by the property in Hypermesh. The material is input in the component by material card which is read by LS Dyna solver.

Figure 4: Roof and Roof Reinforcement Model

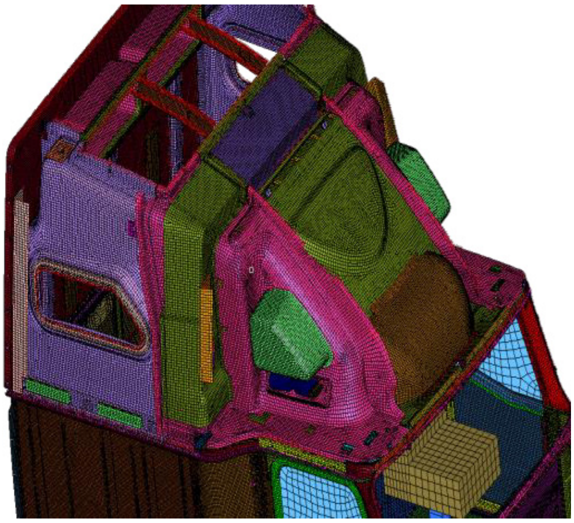

ROOF STRENGTH ANALYSIS

Finite Element Modeling Set Up

Figure 5 shows the FE model of the new cab mount on both frame and cab side. The element used to mesh cab mount is hexahedral element. The hexahedral element has 3 DOF.

The cab mount assembly is then connected to the Cab in white with rigid elements. The rigid elements are constrained in all 6 DOF's.

The Cab in white is modeled using 2D shell elements. Bolts, spring, spot welds are modeled using 1D rigid elements. Dummy is assigned rigid material MAT20.

The side and top platen was modeled as rigid and the rest of the model as deformable. The non-linear material properties for the steel parts were defined using.

*MAT_PIECEWISE_LINEAR_ PLASTICITY card. Contact between the CIW and side platen was defined using the *CONTACT_AUTOMATIC_SINGLE_SURFACE card.

Units Used

Mass : kg

Time : ms

Length : mm

Force : kN

Figure 5: FE Model of New Front Mount Design

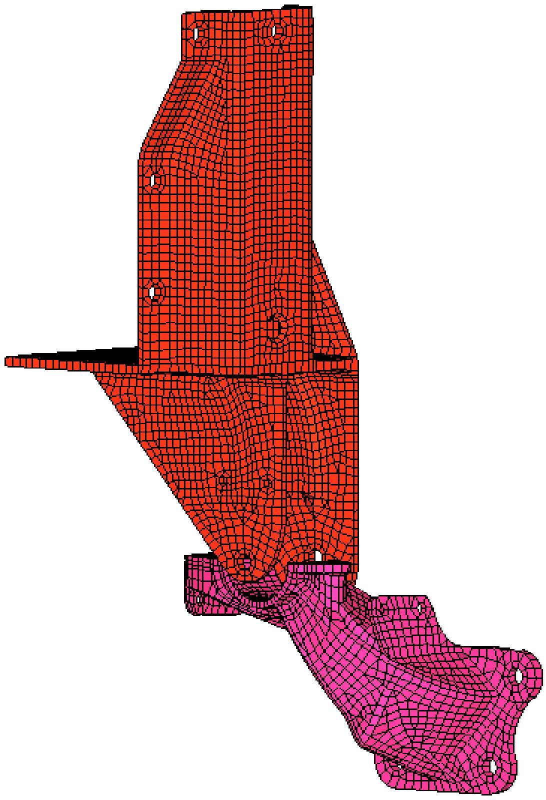

Loads and Boundary Condition

The FE model is constrained at the cut section of the front mount in all DOF's. Similar constraint is applied at the rear mount. The CIW is deformable i.e mate-rial used is elastic plastic. The material type used is MAT24, piece wise linear elasticity.

Figure 6: Loads and Boundary Condition

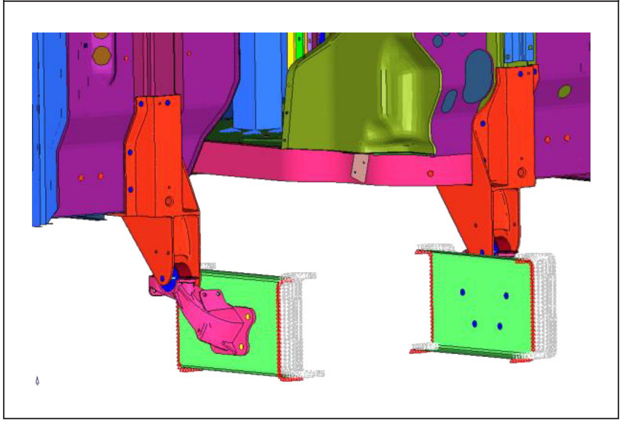

Finite Element Model Set Up for Phase I and Phase II

Figure 7 shows the boundary condition in phase I. In this phase total energy of 18550 is imparted to the side platen. Initial velocity of 2.2 mm/msec is given to the rigid impactor along the direction normal to the platen. The cab is titled about 20 degree to the vertical axis. The energy from the rigid platen is transferred to the cab. The analysis in phase I is dynamic in nature.

Figure 7: Loads and Boundary Condition of Phase I

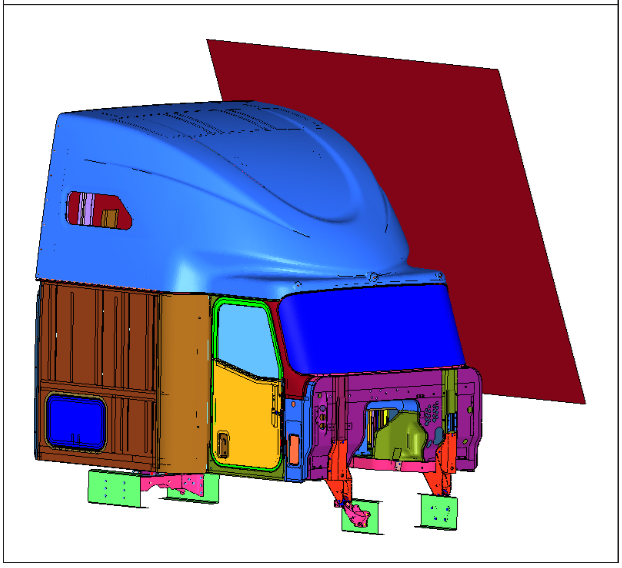

Figure 8 shows loading in phase II. This phase is a continuation of phase I. The analysis is quasi-static in nature. The total load of 1.05 times 12600 lbs or 14330 lbs i.e. 68.2 kN which is the front axle weight is applied to the top platen. The cab has to hold this load with adequate survival space to meet FMVSS 216.

Figure 8: Loads and Boundary Condition of Phase II

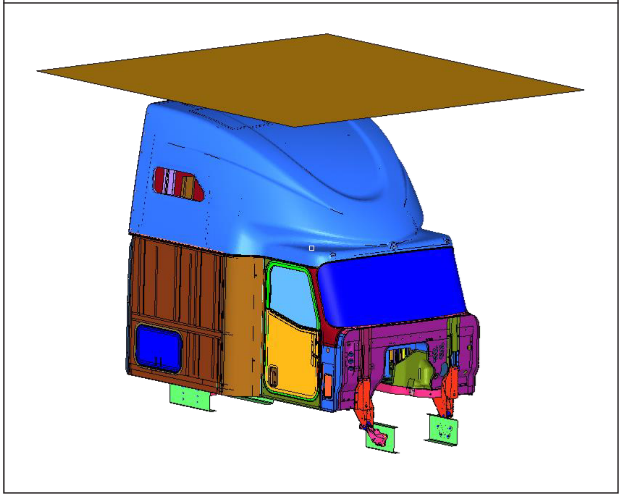

Acceptance Criteria FMVSS 216 and ECE R29 requires the cab roof to withstand a static load equivalent to the front axle mass rating up to a maximum of 10 tonnes (22,046 lbm). After loading, the cab must provide adequate survival space as determined by placing a manikin of prescribed dimensions inside the cab in a prescribed manner without contact between the manikin and non-resilient parts of the cab. The cab must remain attached to the chassis frame, and the doors must not open during the test.The cab should sustain 105% of the load per FMVSS 216. Intrusion into the occupant is not permitted. The FAWR is 14,600 lbs. Hence, acceptance load is 105% of 14,600 lbs or 69.4 kN. The simulation should run to 105% of the 14.6k FAWR.

Analysis results During phase I, the whole cab tilts laterally considerable due to the front and rear cab mount damping properties. The cab rebounds after phase I and tries to retain its original position, but not completely. Permanent set in seen in some panels of the cab e.g. firewall, back panel, floor pane, roof etc. Figure 9 shows the strain contour at the firewall. The maximum plastic strain seen on the firewall is 28% which is very localized, whereas the allowable plastic strain is 15%.

Figure 9: Strain Contour Seen on Firewall at 105% of 14.6k Load

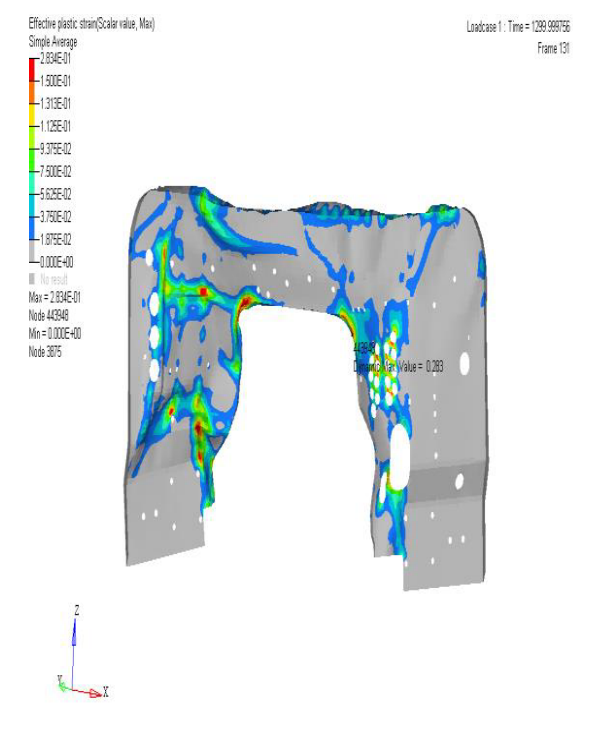

During phase II, the roof deforms. Figure 10 shows the strain contour of the back panel. The maximum plastic strain seen on the roof is 21% whereas the allowable plastic strain is 8.6%, so some local damage is predicted. Figure 11 shows the strain contour of the back panel reinforcement.

Figure 10: Strain Contour Seen on Back Panel at 105% of 14.6k Load

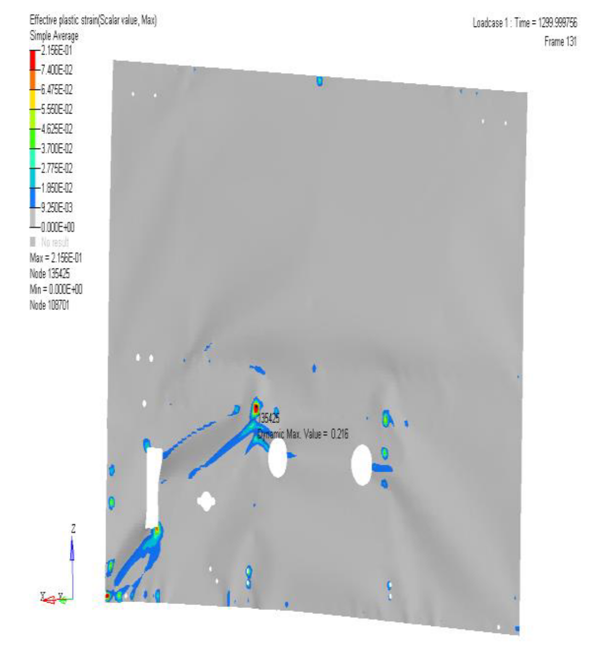

The maximum load during phase I is being transferred to the front mount. The cab tilts 45 degrees to the left where the maximum force is transferred to the front mount. Maximum force of 20 kN could go into both the front mount.

Figure 11: Strain Contour Seen on Back Panel Reinforcement

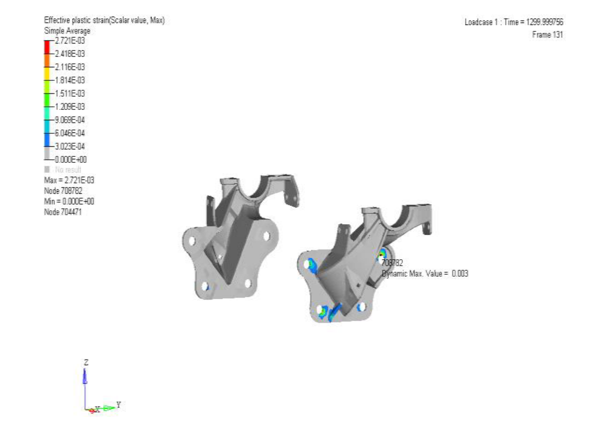

The maximum plastic strain seen on the front mount frame side is 0.5% whereas the allowable plastic strain is 10%. Hence, the revised front mount casting is predicted to hold the applied load.

Figure 12: Loads Curve Used in Phase I for the Rigid Top Platen

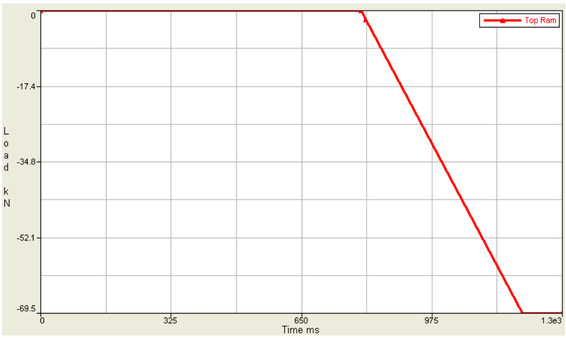

Figure 13 shows that the load versus time plot absorbed by the top platen which is equal to the applied force, an indicator of a successful simulation. The plot show that the maximum reaction force is 68kN. This final load is 105 % of 68.5 kN.

During the first phase the load is not applied for 700 ms. The load is then ramped up to 68.5 kN in phase II.

Figure 13: Reaction Force Plot Seen Between Cab and Platen During Phase I and II

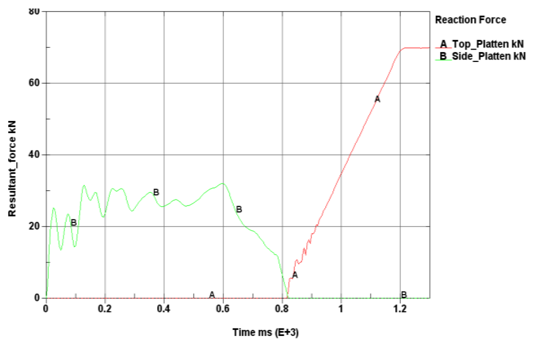

The reaction is measured from the RC contact in Dyna, which is given by surface to surface. The gaph is plotted in Hyperview. The green line shows a reaction force of 30 kN where as the red line denotes the reaction between top rigid platten and the cab in white. The energy in the system has stabilized for 105% of FMVSS 216 load (Figure 14) an indicator that the cab holds the FMVSS 216 load. The total energy at the end of the simulation is constant. This shows that the energy in the system has stabilized. The internal energy is the work done to overcome the strain in the material. As work done is force X displacement. Initially the kinetic energy is very high but tends to zero at the end of the analysis.

The hourglass energy is minimal which shows that the mathematical model has no convergence issues and there are no zero energy modes. There are no elements in the model which is not giving reaction to the applied load.

Figure 14: Energy Plot Showing that the Analysis has Stabilized

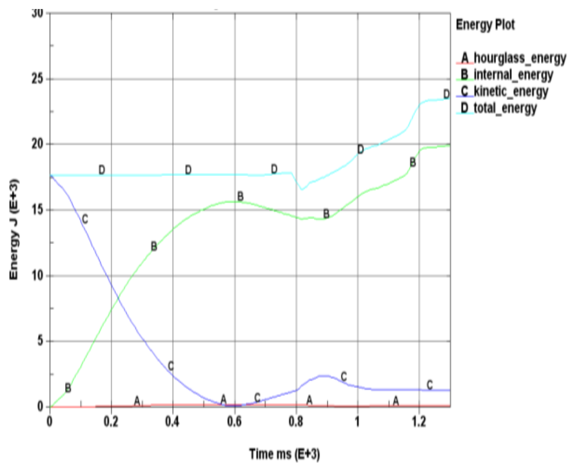

The other energies in the system like sliding interface energies are minimal, showing that the system has stabilized. It is very important to know that the stabilization of these energies is essential to the solution as they are indicators that the mathematical model has stabilized or has converged. Various contact such as surface to surface automatic and node to surface contact has been used. The co-efficient of dynamic friction is 20% more that co-efficient of static friction. These values can be varied as the surface requirement. In this problem it has been kept as F.S = 0.12 and F.D = 0.1.

Figure 15: Survival Space of the Occupant

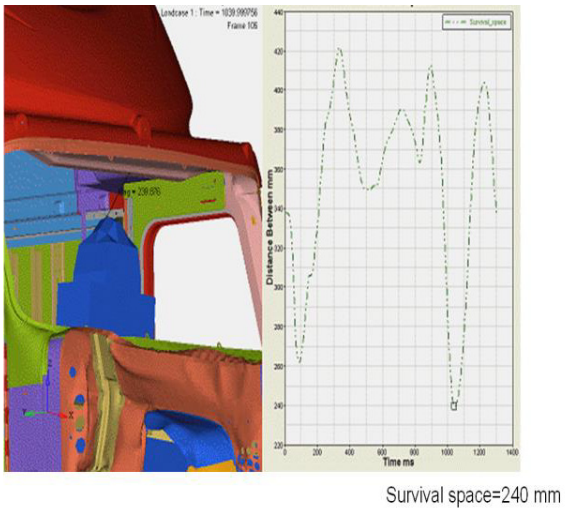

Figure 15 shows minimal survival space of 240 mm after 105% 14.6k load as. This space is measured between door header trim parts to the nearest point of the occupant. The final distance between the nearest part of the CIW to the occupant is approx. 340 mm which is almost same to the measured value of 350mm during testing. A plot of relative distance to time is plot in the graph as well. The intrusion of the components or parts into the cabin space is checked during the analysis. From the analysis results we see that during phase I the maximum deformation is seen at the firewall and in phase II the maximum deformation is seen at the roof. Both these deformation are far away from the occupant intrusion. Hence, we could conclude that the cab with the revised chassis-side front cab mount casting is predicted to meet the requirements of FMVSS 216 and ECE R29 for up to 14.6k FAWR. 4. CAE and Test Co-relation Co-relation The most important parameter observed is deformations and the deformation pattern is observed at the back panel. Figure 16 shows the buckling of the back panel after phase II. Similar deformation pattern is observed in CAE analysis as well.

Figure 16: Test and CAE co-relation Seen at Back Panel

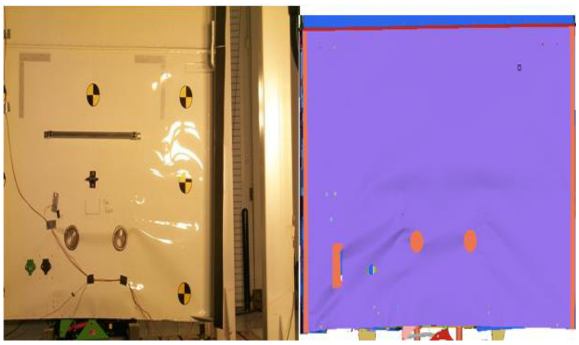

This deformation shows that the CIW can take the 68.5 kN load. Further analysis could be been done for a higher rating axle without testing. CAE result would be 5 percent away from test results. To begin with it can be a very good methodology As seen in the test report the engine tunnel as well as the firewall shows parrellogrammed deformation or failure.

Figure 17 shows similar lateral bending of the firewall during test and similar deformation pattern in CAE analysis. Cracks have observed at the cab mount during this phase. The failure is mainly due to the impact loading in phase I.

Figure 17: Test and CAE Co-relation Seen at Firewall

The engine tunnel opening parallelogrammed, pulling a Huck bolt and rivet through the adjacent sheet metal at the left rear of the tunnel.

Figure 18: Test and CAE Co-relation Seen at Roof

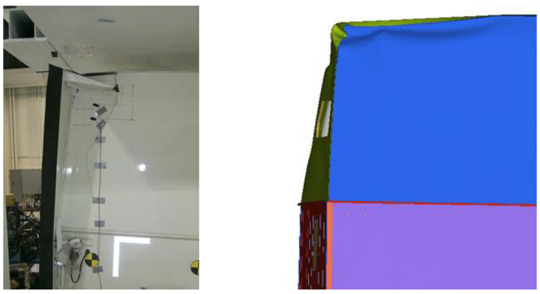

Figure 18 shows failure at the roof after phase II when the top platen is loaded on the roof. This failure is also seen in CAE analysis. Strain seen on the roof is about 7-8% which is higher than its allowable strain for FRP material of 4 %.From these figures it shows that the physical test and CAE results are in good agreement to each other.

Hence we can conclude that good co-relation between physical test and CAE has been obtained. This CAE or mathematical model could be used for higher rating axle load for different cab configuration.

CONCLUSION

- The cab with the revised chassis-side front cab mount casting is predicted to meet the requirements of FMVSS 216 & ECE R29 for up to 14.6k FAWR as survival space seen is more that 240mm whereas the acceptance criteria is about no intrusion into the occupant.
- The new cab mount design with ADI material passes the strength requirement for FMVSS 216

REFERENCES

1. Altair (2012), "HyperStudy 12.0 User's Guide", *Altair Engineering, Inc*.
2. Huang L, Kuo M and Yan B (2007), "AHSS Application in Roof Strength", *SAE Technical Paper*.
3. Laxman S, Iyengar R M and Morgans S (2009), "Achieving Light-Weight Design of Automotive Bodies with Advanced High Strength Steels via Structural Optimization", *SAE Technical Paper*.
4. Pathare R and Mansour M (2009), "Automotive Roof Crush, Structural Foam Enhancement Solution", *SAE Technical Paper*.
5. Shaw J, Engl B, Espina C and Oren E C (2002), "ULSAB Advanced Vehicle Concepts - Materials", *SAE Technical Paper*.